Fundamental parameters of nearby stars from the comparison with evolutionary calculations: masses, radii and effective temperatures[*]

C. Allende Prieto and D.L. Lambert

McDonald Observatory and Department of Astronomy, The University of Texas at Austin, RLM 15.308, Austin, TX 78712-1083, USA
(callende, dll@astro.as.utexas.edu)

Abstract. The *Hipparcos* mission has made it possible to constrain the positions of nearby field stars in the colour-magnitude diagram with very high accuracy. These positions can be compared with the predictions of stellar evolutionary calculations to provide information on the basic parameters of the stars: masses, radii, effective temperatures, ages, and chemical composition. The degeneracy between mass, age, and metallicity is not so large as to prevent a reliable estimate of masses, radii and effective temperatures, at least for stars of solar metallicity. The evolutionary models of Bertelli et al. (1994) predict those parameters finely, and furthermore, the applied transformation from the theoretical ($\log g - T_{\rm eff}$) to the observational (M_v–B–V) plane is precise enough to derive radii with an uncertainty of $\sim 6\%$, masses within 8%, and $T_{\rm eff}$s within $\sim 2\%$ for a certain range of the stellar parameters. This is demonstrated by means of comparison with the measurements in eclipsing binaries and the InfraRed Flux Method.

The application of the interpolation procedure in the theoretical isochrones to the stars within 100 pc from the Sun observed with *Hipparcos* provides estimates for 17,219 stars.

Key words: stars: fundamental parameters – stars: luminosity function, mass function – stars: Hertzsprung–Russel (HR) and C-M diagrams – Galaxy: stellar content

1. Introduction

Stellar evolution calculations for single stars model their evolution in terms of the variations of their fundamental parameters R and $T_{\rm eff}$, as a function of time since the starting of hydrogen fusion reactions until their final extinction. Mass is the key parameter that decides the stars' evolution, chemical composition and other factors play a secondary role. The evolution of the stars can be plotted as tracks in the HR diagram, some of its areas being more crowded by paths corresponding to stars of different masses. Other regions are completely empty, forbidden spaces which no star is supposed to cross.

At least in principle, after proper conversion from the theoretical to the observational plane, it is possible to associate the position of a star in the HR diagram with a given stellar mass and time since its birth, or with a range of masses and times. The only requirements are an accurate knowledge of the distance from the observer to the star, and a pair of photometric measurements. This is a well-known method that has been largely applied to simplified cases where some constraints on age and distance exist, such as well detached binaries or stellar clusters. It has also been used in the search for age-metallicity relationships in the Galactic Disc or the Halo. Most of the stellar parameters at play in the calculations are the very same that define the atmospheric properties, and so shape the features observed in the stellar spectra. These quantities have been often estimated directly from the spectra, and only in a few situations, commonly for the lack of empirical alternatives, has consideration been given to the evolutionary models.

Before trying to apply the method, several important questions need to be posed, such as how crowded is the HR diagram, or in other words how severe is the degeneracy between age, mass and metallicity for a given position in the HR diagram. It is of relevance to demonstrate that the translation from the theoretical parameters to the observational plane is properly done, otherwise no matter how realistic the calculations are, there is no hope to get useful results. Finally, an extensive assessment of the adequacy of the evolutionary calculations is required. All three issues can be simultaneously answered in applying the method to several favourable cases. Stellar masses and radii are known with extremely high accuracy for a bunch of nearby eclipsing binaries (Popper 1980; Andersen 1991). Some of these systems have been already employed by Schröder et al. (1997) and Pols et al. (1997) to test critically their evolutionary calculations (Pols et al. 1997) and tune parameters in their scheme that take account of convection. Stellar radii are alternatively and independently measured by interferometric techniques (e.g. Richichi et al. 1998) and also by the so-called InfraRed Flux Method (Blackwell & Lynas-Gray 1994). The later provides probably the most direct and model-independent estimate of the stellar effective temperature. Other parameters involved are the chemical composition and the age. Although it is possible to check the metallicity estimates from the isochrones with the results from spectroscopic measurements, and the stellar ages can be
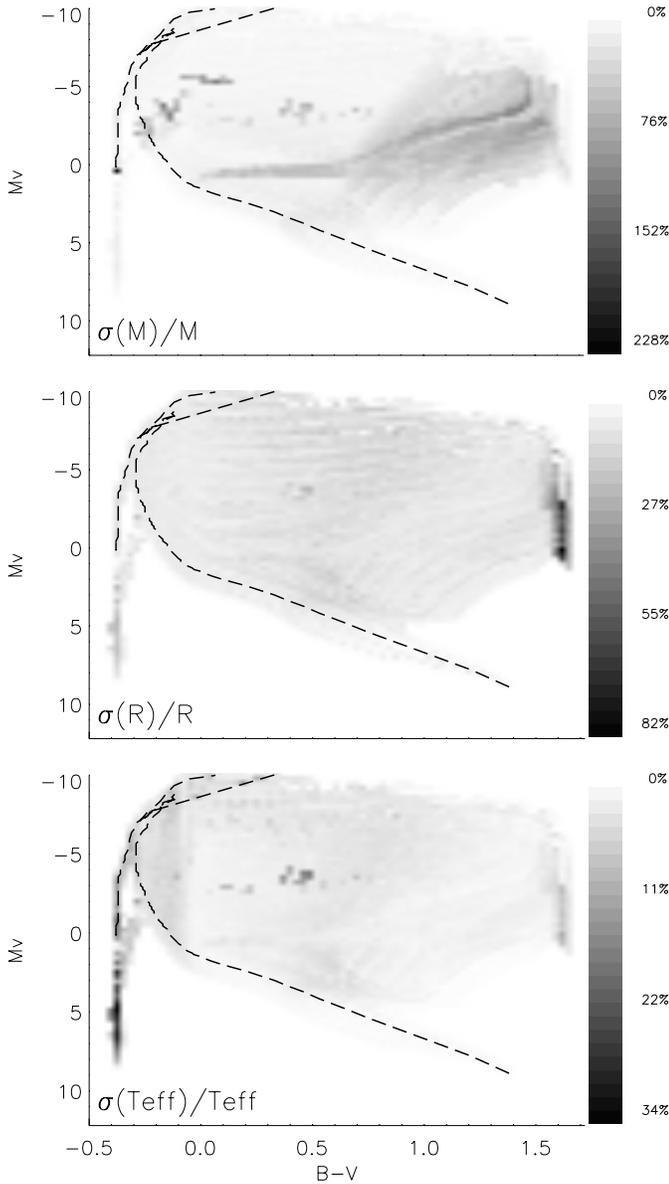
Fig. 1. Uncertainties in the colour-magnitude diagram indicating the confusion for the masses, radii and effective temperatures retrieved for a given star based only on its position in the diagram. The dashed line represents an isochrone of solar metallicity and 4 Myrs.

compared with other methods, such as activity indicators (see, e.g., Rocha-Pinto & Maciel 1998), or the abundances of radioactive nuclei (see, e.g., Goriely & Clerbaux 1999), we shall not concentrate on them here.

In this paper, we have made use of the stellar evolutionary calculations of Bertelli et al. (1994) to study the possibility of retrieving the fundamental stellar parameters: radius, mass, and effective temperature, from the comparison of the stars' position in the colour-magnitude diagram with computations of stellar evolution for isolated stars. We quantify the degeneracy between mass and age for a given place in the HR diagram using error bars in the estimates of these parameters. Stars in eclipsing binary systems and the InfraRed Flux Method are used to test

the procedure. And finally, the technique is applied to 17,219 stars identified by the *Hipparcos* astrometric mission within an sphere with radius of 100 pc centred in the Sun.

2. Retrieval of the stellar parameters. Interpolation in the theoretical isochrones

Calculations of stellar evolution interpolated to find the position of coeval stars of a given chemical composition but different masses are commonly referred to as isochrones. Among the published isochrones, those presented by Bertelli et al. (1994) span all observed stellar masses, metallicities from [M/H] = -1.7 to 0.4, and stellar ages from 4×10^6 to 2×10^{10} yrs. The computations mostly use the OPAL radiative opacities by Rogers & Iglesias (1992) and Iglesias et al. (1992). The reader is referred to Bertelli et al. (1994) and references therein for details.

We assume that both the B$-$V colour, and the absolute magnitude (and therefore the distance to the star) are known with enough precision to avoid significant observational errors affecting derived quantities. We quantify this statement below. To retrieve the appropriate set of stellar parameters that reproduces the position of a star in the colour-magnitude diagram we proceed as follows. First we search the entire set of isochrones to find what are, if any, the B$-$V colours that reproduce the observed absolute V magnitude (M_v) within the observational errors. Then, the different possible solutions, corresponding to different ages, metallicities, masses, etc. are averaged to obtain a mean value for every stellar parameter, and an estimate of the uncertainty from the standard deviation.

The final uncertainty includes three components. First of all, the intrinsic spread, as different evolutionary paths cross the same area of the colour-magnitude diagram. Second, the noise introduced in the translation from the theoretical $\log g - T_{\mathrm{eff}}$ plane to the observational colour-magnitude diagram. Also, observational errors in the two considered parameters (B–V and M_v) contribute. Applying the procedure along a grid of colours and absolute magnitudes, we construct maps of the combined uncertainties expected for the different stellar parameters. We are mainly interested in radii, masses, and T_{eff}s: the magnitudes available from observations of eclipsing binaries and the IRFM we are comparing to in the subsequent sections. The gray scale in the images included in Fig. 1 has been set to represent the relative uncertainties in these magnitudes. To construct the maps we have assumed an uncertainty of 0.01 dex in B–V and of 0.2 dex in M_v. The dashed line indicates an isochrone of 4 Gyrs. and solar chemical composition. The largest errors correspond to the darkest areas: $\sim 200\%$ for the mass, $\sim 80\%$ for the radii, and $\sim 30\%$ for the effective temperatures. Uncertainties in the retrieved masses are especially significant close to the position of the horizontal branch, where intermediate mass stars cross back from the giant stage and more massive stars make their way up from the main sequence, and reach the worst expectations for giants and AGB stars. Understandably, there is also significant confusion in the area where the post-AGB stars cross the upper main sequence way down to the white dwarf cooling sequence,

although in practice very few stars will appear in such a rapidly evolving phase. Errors in the retrieved radii are small for most of cases, although for the reddest evolved stars the confusion is very large, and a similar conclusion is sketched from Fig. 1 for the effective temperatures.

These results show that radii and T_{eff}s, are largely constrained by the position of a star in the colour-magnitude diagram, regardless of the existence of a wide range of possibilities for ages and metallicities. It is apparent from Fig. 1 that the masses of evolved stars with different ages and metallicities show more disparate values at a given position in the colour-magnitude diagram.

3. Critical testing

Highly reliable measurements of stellar masses and radii are available for eclipsing binary systems. We use them to check the method suggested here for deriving the fundamental stellar parameters from the comparison between the position of the stars in the colour-magnitude diagram and the predictions of stellar evolution calculations. The model-independent effective temperatures and stellar diameters obtained through the InfraRed Flux Method by Blackwell & Lynas-Gray (1994) for solar-metallicity stars are also used in the test.

3.1. Eclipsing binary systems

No doubt these privileged binary systems can provide the most solid determinations of stellar masses and radii. Andersen (1991) has produced the most recent compilation of high-accuracy ($< 2\%$) determinations in binaries, listing 90 stars. Andersen lists errors for the absolute V magnitudes, and we have assumed errors in the B–V colour to be 0.01 dex.

The upper and middle panels of Fig. 2 compare the differences between the direct estimates of radius, and mass with those retrieved from the interpolation in the isochrones. The dashed lines correspond to differences of $\pm\,10\%$. The radii are accurately well predicted with a remarkable standard deviation of 6%. The masses show a larger scatter of $\sim 12\%$. Note that in these two panels of Fig. 2, the horizontal axes have been logarithmically expanded for clarity. The effective temperatures listed by Andersen (1991) come from different estimators. However, it is important to remark that spectroscopic analyses of these systems normally combine photometry and spectroscopy, and then the effective temperatures are likely to be more reliable than those in most of studies of isolated field stars. The mean of the relative errors in the effective temperature provided by Andersen for his sample is 3%. The lower panel of Fig. 2 shows the comparison with the effective temperatures retrieved from the evolutionary models. The agreement is excellent: the standard deviation is a mere 4%.

For a given position in the colour magnitude diagram, radius and luminosity (and therefore, effective temperature) depend very weakly on metallicity. However, that does not apply to mass and it is reflected in Fig. 1 through the large uncertainties for the retrieved masses. The fact that the stars in the Andersen
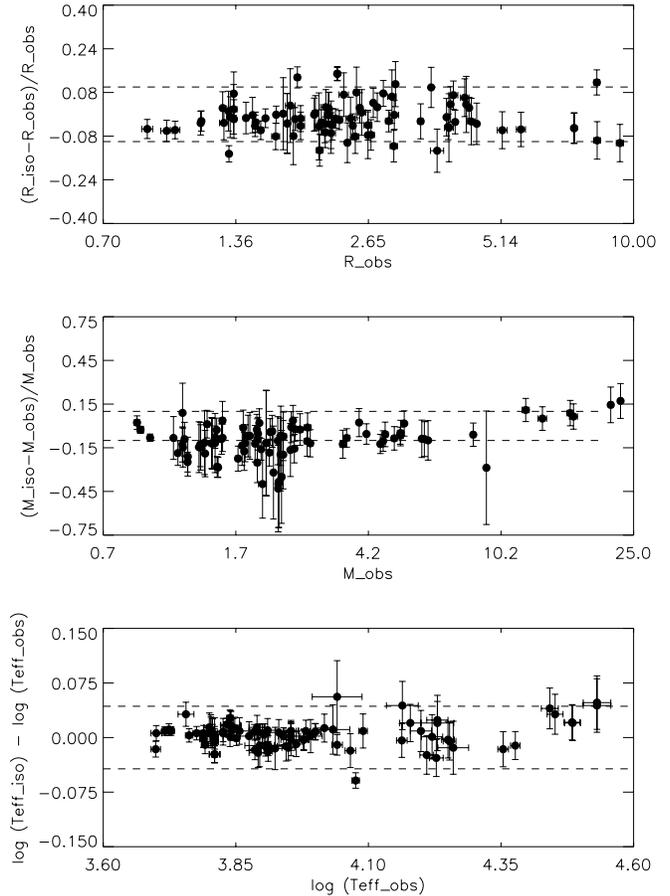

Fig. 2. Relative differences between stellar radii, masses and T_{eff} derived from stellar evolutionary calculations and the robust direct estimates from observations in eclipsing spectroscopic binaries compiled by Andersen (1991).

sample are all nearby, and therefore are roughly of solar metallicity is very useful to demonstrate this feature. Fig. 3, represents a comparison of the same magnitudes as in Fig. 2, but now the masses, radii, and T_{eff}s, have been estimated assuming roughly solar metallicity ($-0.7 <$ [Fe/H] $< +0.4$), and then further restricting the set of isochrones. The agreement between observed and predicted radii improves very little, as reflects the standard deviation of 5%, and no significant improvement is achieved in the effective temperature, but the tendency to underestimate some of the masses no longer exists: the standard deviation of the relative differences between predicted and observed masses is now reduced to 8%. These results indicate that the combination of these masses and radii will lead to gravities estimates with a standard deviation in $\log g$ of 0.06 dex. For low-gravity stars of solar metallicity, a smaller mass will be derived by assuming the star to be metal-poor, and then the average of all metallicities underestimate the true value, as shown in Fig. 2.

(Z) for the two components of the binary systems of Andersen (1991).

Only one of the stars in Andersen's sample (TZ For A) has a gravity lower than $\log g = 3$ and hence the sample is restricted to objects on, or close to the main sequence. To avoid
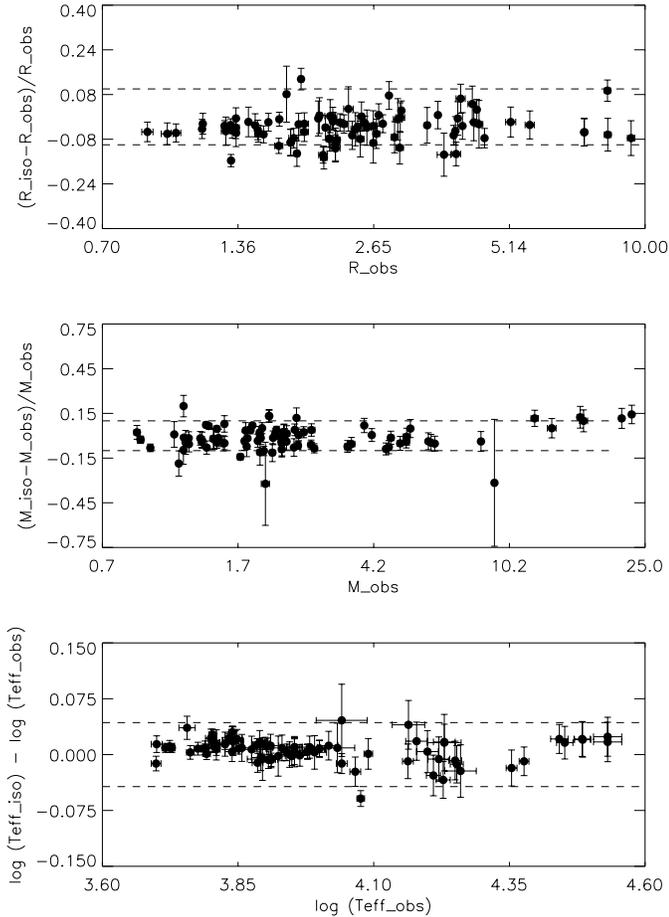
Fig. 3. Relative differences between stellar radii, masses and T_{eff} derived from stellar evolutionary calculations assuming roughly solar metallicity ($-0.4 < [\text{Fe/H}] < +0.4$) and the direct estimates from observations in eclipsing spectroscopic binaries compiled by Andersen (1991).

Fig. 4. Relative differences between stellar radii, masses and T_{eff} derived from stellar evolutionary calculations and the robust direct estimates from observations in eclipsing spectroscopic binaries, against the logarithm of the gravity. The stars compiled by Andersen (1991) have been plotted with filled circles, the two detached subgiant eclipsing systems (Popper 1980) with rhombs, the resolved spectroscopic binaries with open circles (Popper 1980), and the two components of γ Per (Popper & McAlister 1987) and ζ Aur (Bennett et al. 1996) with asterisks.

this restriction we have extended the sample including a few of other systems with somewhat poorer determinations. We have included the 5 resolved spectroscopic binaries compiled by Popper (1980): HD16739, HD168614, δ Equ, Capella, and Spica; and 2 detached subgiant eclipsing systems: TY Pyx and Z Her, also included in the compilation by Popper. The sample was completed with the studies of ζ Aur by Bennett et al. (1996) and γ Per by Popper & McAlister (1987). The B–V for the two components of γ Per have been estimated from their spectral type and the tables of Aller et al. (1982).

T_{eff}s are provided for the stars in these systems, the resolved spectroscopic binaries with open circles, and the two components of γ Per and ζ Aur with asterisks. Fig. 4 shows no correlation of the relative differences between *observed* and *evolutionary* radii, masses, or effective temperatures against $\log g$.

3.2. The IRFM

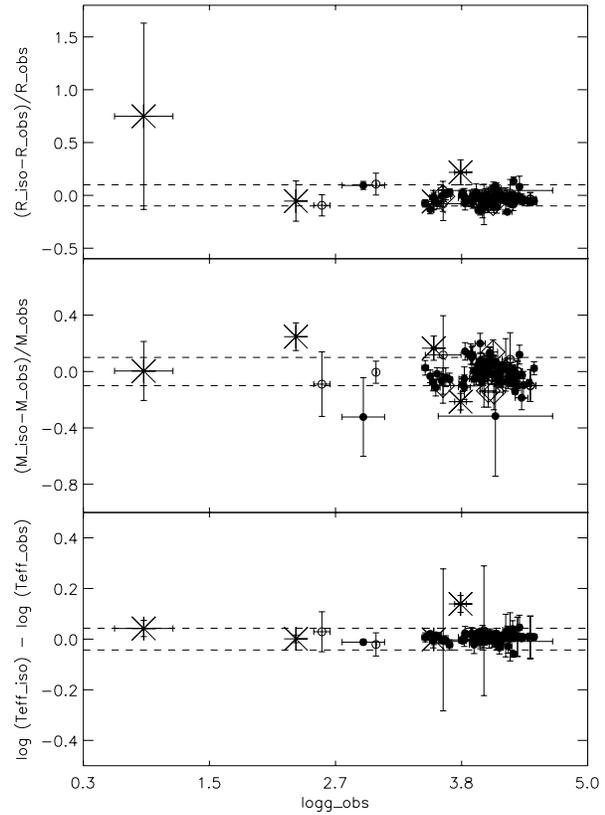The InfraRed Flux Method, developed by Blackwell and his collaborators, provides an accurate procedure to derive stellar angular diameters and effective temperatures by measuring the monochromatic flux at an infrared frequency and the bolometric flux, and using theoretical model atmospheres to estimate the monochromatic flux at the star's surface. The method has been applied by Blackwell & Lynas-Gray (1994) using the Kurucz (1992) LTE model atmospheres to a sample of 80 stars. All but one of the stars in the sample have been observed by the *Hipparcos* mission and we have converted the IRFM angular diameters to radii using the trigonometric parallaxes (π). We have identified the position of the stars in the colour-magnitude diagram making use of the V band photometry and the B−V colours included in the *Hipparcos* catalogue and then interpolated in the Bertelli et al. (1994) isochrones to find the evolutionary status, and the fundamental stellar parameters. One star (HR1325) was rejected, as we could not find an isochrone close enough (within observational uncertainties) to the position of the star in the colour-magnitude diagram. In this analysis, we have neglected the effects of reddening and assumed that the rotational velocities are not high enough to disturb the position of the stars
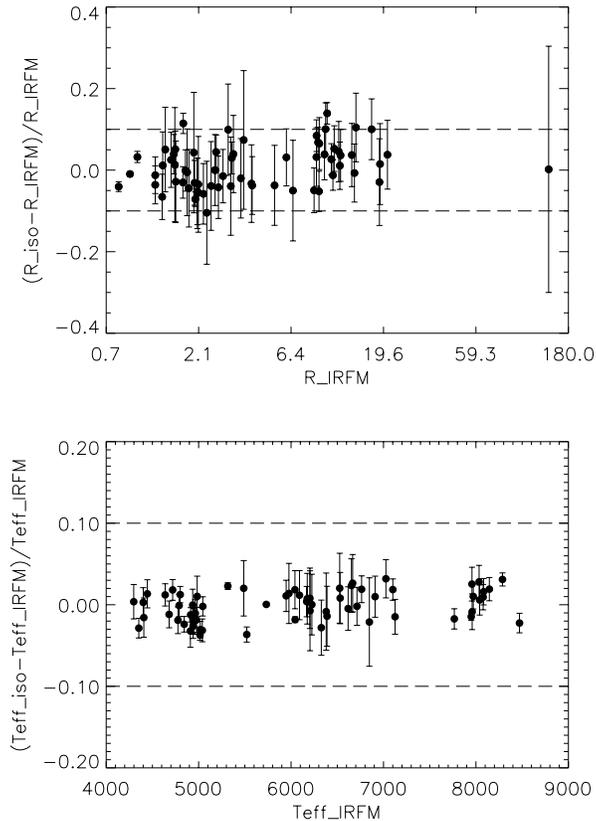
Fig. 5. The relative differences between the radii and $T_{\rm eff}$s derived from stellar evolutionary calculations and those derived from the InfraRed Flux Method (Blackwell & Lynas-Gray 1994).

in the colour-magnitude diagram. No assumption has been made about the metallicity of the sample.

The angular diameters of Blackwell & Lynas-Gray have been converted to radii using the Hipparcos trigonometric parallaxes. The upper panel of Fig. 5 shows the comparison between the derived radii against the estimates from the evolutionary models. Again, the agreement is gratifying showing a standard deviation of only 5%. The effective temperatures retrieved from the isochrones are also compared to the IRFM temperatures in the lower panel of Fig. 5. The standard deviation of the comparison is less than 2%. The sample includes a star as far as 277 pc from the Sun, a distance at which errors in the *Hipparcos* parallax are expected to be significant, but the rest of the stars are within 100 pc.

The radius of the largest star in the sample (HR2473; G8Ib) from the IRFM measurements is about 142.0 $R_\odot$, in good agreement with the prediction from its position in the colour-magnitude diagram 142.3 $R_\odot$ (see Fig. 5). However, such a highly evolved star, as we previously found for the cool component of ζ Aur, occupies a region in the red part of the colour-magnitude diagram quite crowded by stellar evolutionary tracks, ending up with a very large uncertainty in the retrieved stellar parameters (see Fig. 1). In the case of the radius, the standard deviation is 43 $R_\odot$. The difference here from the previous comparison for the K supergiant in ζ Aur is that for HR2473, the

mean value of the radii compatible with the star's position in the colour-magnitude diagram is in very good agreement with the observational estimate.

4. Application of the method to the Hipparcos catalogue

Taking into account both the accuracy of the estimates and the the range of parameters where the predictions are too vague (*crowded* zones in the colour-magnitude diagram), the stellar evolutionary calculations can be used with no more than photometry and the trigonometric parallax within the following limits:

$$\begin{aligned}
0.87 &\leq R/R_\odot &\leq& \quad 21 \\
0.88 &\leq M/M_\odot &\leq& \quad 22.9 \\
3{,}961 &\leq T_{\rm eff} &\leq& \quad 33{,}884 \text{ K} \\
2.52 &\leq \log g &\leq& \quad 4.47.
\end{aligned} \tag{1}$$

The samples used here to test the accuracy of the procedure to retrieve the stellar parameters are strongly biased towards solar metallicities. We have shown that the comparison between *physical* and predicted values is excellent when restricting the possible range for the metallicity to roughly solar ($-0.4 <$ [Fe/H] $< +0.4$), based on *a priori* knowledge of the statistical peculiarities of the sample. Nevertheless, the results here described cannot be safely extended to low-metallicity stars without further study.

A precise knowledge of the fundamental stellar parameters is essential to make a comparison possible between observations and theoretical studies, shedding light on multiple aspects of stellar structure, stellar evolution, and the physics of stellar atmospheres. From the previous sections, we have seen that it is possible to use in a direct manner the isochrones of Bertelli et al. (1994) to estimate masses, radii, and effective temperatures for unevolved stars with solar-metallicity provided an accurate estimate of the distance from Earth is available. The *Hipparcos* mission has measured, among other quantities, parallaxes that lead to distances precise typically better than 20% up to 100 pc from the Sun (see, e.g., Perryman et al. 1995). We have derived absolute magnitudes and combine them with the B–V index (compiled also in the *Hipparcos* catalogue) to estimate masses, radii, gravities, and effective temperatures for 17,219 stars that appear within the range of masses, radii, and gravities assessed in this study out of 22,982 stars included in the *Hipparcos* catalogue within the sphere of 100 pc radius from the Sun. Solar metallicity ($-0.4 <$ [Fe/H] $< +0.4$) has been assumed. Although the tail of the metallicity distribution of stars in the solar neighbourhood reaches [Fe/H] $\simeq -1$, most of the stars are within the selected interval (Rocha-Pinto & Maciel 1996).

An overview of a few of the possible uses of these data is given in the next section. Table 1, available only in electronic format, includes the following information: *Hipparcos* #, V, π, $\sigma(\pi)$, M_v, $\sigma(M_v)$, B–V, $\log g$, $\sigma(\log g)$, $M/M_\odot$, $\sigma(M/M_\odot)$, $\log(R/R_\odot)$, $\sigma(\log R/R_\odot)$, BC, $\sigma(BC)$, $\log T_{\rm eff}$, and $\sigma(\log T_{\rm eff})$. Fig. 6 shows the derived luminosity and actual mass functions for the sample. These figures have been derived using the data in Table 1, and therefore are restricted to the
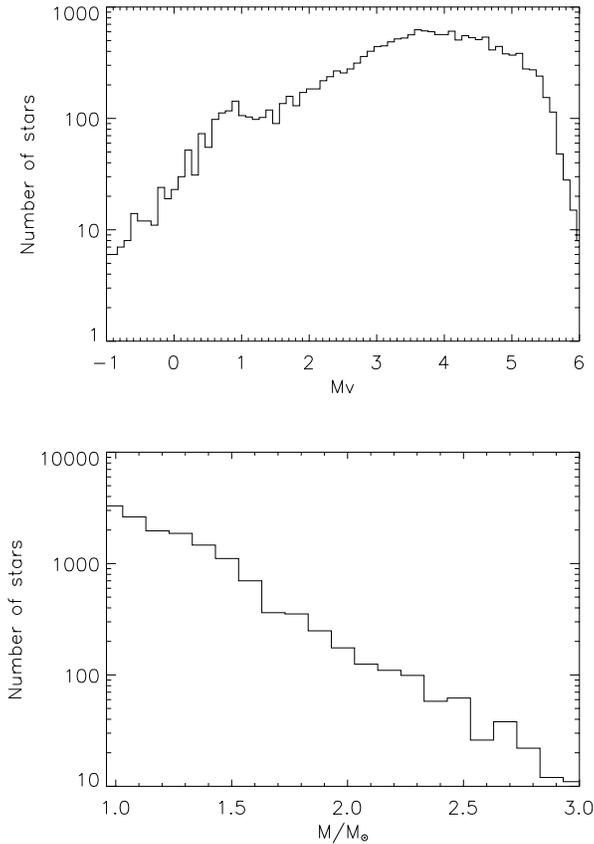
Fig. 6. Luminosity function (upper panel) and mass function (lower panel) for the sample studied.

range $0.8 \leq M/M_\odot \leq 22$, although the statistics are poor for the more massive stars and we have further restricted the plots. Although it is beyond the scope of this paper, the study of these distribution functions will likely shed light on the discussion about the universality of the initial mass function, and the star formation history of the Galactic disc. The use of a finer grid for the interpolation in stellar age and metallicity may provide additional information.

5. Discussion of the results

The comparison between the stellar masses, radii and effective temperatures for detached eclipsing binaries and those analyzed by the IRFM with the values retrieved from the position of the stars in the colour-magnitude diagram and interpolation in the isochrones of Bertelli et al. (1994), showed that the latter provides a method to estimate those fundamental parameters with high accuracy for most purposes. Stellar radii can be predicted to $\sim 6\%$, masses to $\sim 8\%$, and effective temperatures to $\sim 2\%$ for the ranges in these parameters listed in Sect. 4.

However, the longest episode in stellar evolution, the main-sequence, imposes a bias in the samples. Giants and super-giants are not common in the analysed samples with high-quality data, and hence our conclusions cannot be safely extended to very low gravities. New observational efforts are in progress (see, e.g. Bennett et al. 1998) and are likely to improve the situation

in the future. The same or very similar arguments apply to the metal content of the stars. Our sample is biased towards solar-like metallicities and from the material studied here it is not possible to derive any conclusion for the lower-metallicity domain. The addition of more constraints, such as prior (from spectroscopy or photometry) knowledge of the stellar metal abundance, and a more detailed analysis, weighting the different possible stellar models with care, depending on the speed with which they cross that part of the colour-magnitude diagram, should likely improve the results and possibly extend its applicability to metal-poor stars.

Rotation changes the position of the stars in the colour-magnitude diagram (Maeder & Peytremann 1970). Typically, the position of a star rotating at $\sim 200\,\mathrm{km\,s^{-1}}$ will change by 0.1–0.3 mag in M_v and 200–250 K in T_{eff}. Therefore, for high rotational velocities, has to be taken into account before applying the procedure described here.

It is possible to get better B–V colour estimates than those compiled in the *Hipparcos* catalogue. The calibration of Harmanec (1998) makes it possible to accurately estimate the V and B colours from the B−V and U−B indices together with the *Hipparcos* H_p magnitudes. Besides, the B–V colours listed in the *Hipparcos* catalogue can be refined by combining them with Earth-based measurements, as proved by Clementini et al. (1999).

We have selected the set of isochrones derived from the evolutionary calculations of Bertelli et al. (1994) because they are one of the most homogeneous and comprehensive among those publicly available in electronic format. It is of interest to check whether the use of alternative models would lead to the same conclusions. Considering the particular case of stars between 0.8 and 1.25 $M_\odot$ of 4 Gyr. age, we can compare the calculations of VandenBerg (1985) with those of Bertelli et al. (1994). Fig. 7 displays such a comparison in both, the theoretical ($\log g - T$eff) and observational (M_v- B–V) planes. The points in the isochrones corresponding to equal masses (left-side panels; 0.8, 1.0, 1.25 $M_\odot$) or radii (right-hand panels; 0.83, 1.20, 2.0, 2.51 $R_\odot$) have been linked by solid segments. Differences in the theoretical plane may be the effect of one or more of the different ingredients in the calculations, such as convection treatment or radiative opacities (Los Alamos Opacity Library vs. OPAL), as well as slightly different assumed metallicities (Z=0.0169 vs. 0.02), or mass fraction of helium (Y=0.25 vs. 0.28). The agreement is better for the dwarfs with lower effective temperatures and gets poorer for lower gravities. However, the discrepancies in the observational plane become more significant and systematic, and could induce important differences in the results. Even though there are details such as discordant assumptions for the Sun's bolometric correction (-0.12 vs. -0.08), the different model atmospheres employed in the translation from the theoretical magnitudes must play a major role. The more recent model atmospheres (Kurucz 1992) employed by Bertelli et al. perform adequately, as suggested by the conclusions in Sect. 3.

The positions in the $\log g - T_{\mathrm{eff}}$ plane predicted by the calculations of Schaller et al. (1992) without overshooting, shown
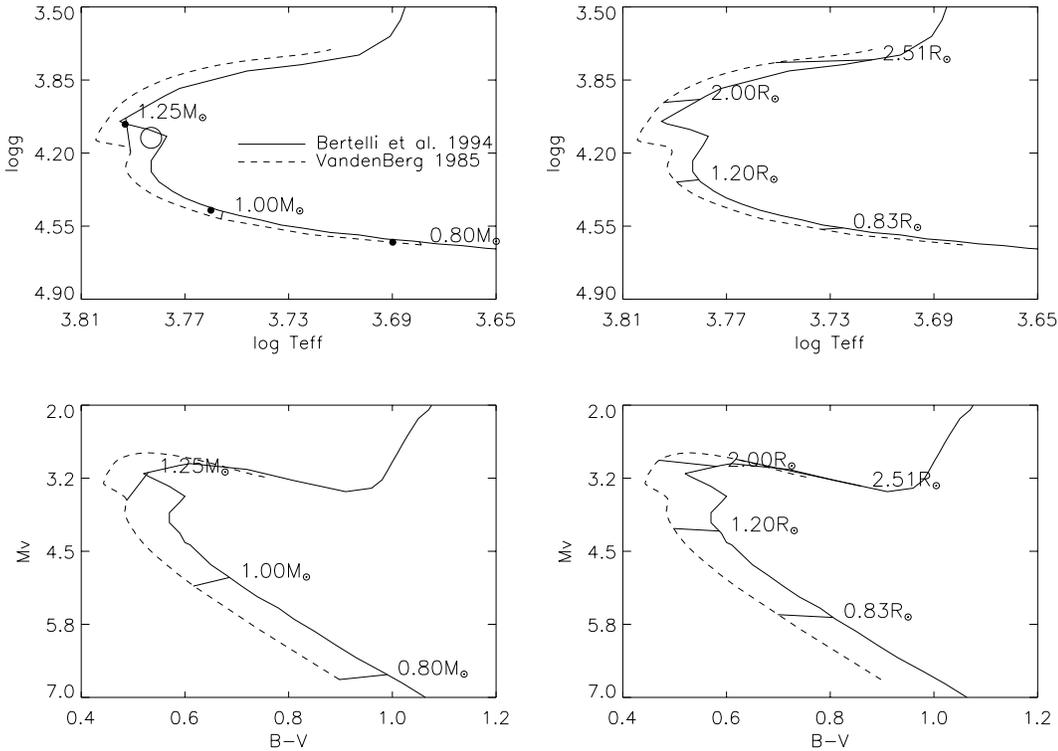
Fig. 7. Differences between the isochrones of Bertelli et al. (1994; solid line) and VandenBerg (1985; dashed line) for solar metallicity and an age of 4 Gyrs. Solid segments join the positions of stars with masses of 0.8, 1.0, and 1.25 $M_\odot$ (left panels) or radii of 0.83, 1.2, 2.0, 2.51 $R_\odot$ (right panels) in both sets of isochrones. The location of stars with the same masses in the theoretical ($\log g - T_{\rm eff}$) plane for the (non-overshooting) calculations of Schaller et al. (1992) are marked with filled circles, including also the case for a 1.25 $M_\odot$ model with overshooting (open circle).

with filled circles in the left-side upper panel of Fig. 7 for 0.8, 1.0, and 1.25 $M_\odot$, do not exactly overlap neither with the predictions derived from Bertelli et al.'s calculations, nor with those of VandenBerg (1985), yet even so they include the same radiative opacities (LAOL; Huebner et al. 1977) and assume the same value for the mixing-length α as VandenBerg's models. Again, slightly different values for $Z_\odot$, $Y_\odot$, and details in the treatment of envelope convection must be responsible. The open circle correspond to a 1.25 $M_\odot$ model with overshooting.

Balona (1994) made use of the calibration of Balona & Shobbrook (1984) to estimate absolute magnitudes from the synthetic Strömgren indices computed by Lester et al. (1986) based on Kurucz (1979) model atmospheres. He derived effective temperatures, gravities, and luminosities from the model atmospheres, and used the $T_{\rm eff}$s and luminosities to interpolate in the models of stellar evolution by Claret & Gimenez (1992) and Schaller et al. (1992) and then estimate *evolutionary* gravities. The comparison showed that the *evolutionary* gravities were larger than the gravities from the model atmospheres for stars with $\log g < 4$, and the discrepancy was increasing towards lower gravities. Besides, the situation appeared to be reversed for stars with $\log g > 4$. The evolutionary calculations used here tend to underpredict the stellar masses for low-gravity stars. However, this effect is much smaller and in opposite sense to the huge differences found by Balona (1994) that were as large as 0.5 dex for $\log g$ (*evolutionary*) ~ 3.5. The explanation is still

unclear, but we note that the comparison of the gravities from LTE (model-atmospheres) spectroscopic analysis (iron ionization equilibrium) with those obtained combining *Hipparcos* parallaxes and evolutionary models seem to agree reasonably well (Allende Prieto et al. 1999; see also Fuhrmann 1998).

Gravitational redshifts are proportional to the mass-radius ratio and systematically affect measurements of stellar radial velocities (Dravins et al. 1999). Photospheric spectral lines are shifted by roughly 600 m s^{-1} for a star like the Sun, and by more than 1000 m s^{-1} for more massive stars in the main sequence. The empirically determined errors for masses and radii derived from the position of a star in the colour-magnitude diagram make it possible to estimate its gravitational redshift with an uncertainty of the order of 100 m s^{-1}.

A precise knowledge of the stellar radius and the distance to the star combine together to translate the measured stellar flux to the flux at the star's surface, a quantity that can be compared with synthetic spectra from model atmospheres. Spectrophotometry is already available for the large sample of stars observed by IUE, HST, and many other missions, and their investigation will likely provide valuable information on the stellar content of the Galactic disc in the solar neighbourhood and beyond.

References

Allende Prieto C., García López R. J., Lambert D.L., Gustafsson B., 1999, ApJ, in press

Aller L.H., Appenzeller I., Baschek B., et al., 1982, Landolt-Börnstein: Numerical Data and Functional Relationships in Science and Technology - New Series, Group 6, Vol. 2, Stars and Star Clusters. Springer-Verlag, New York

Andersen J., 1991, A&AR 3, 91

Balona L.A., 1994, MNRAS 268, 119

Balona L.A., Shobbrook R.R., 1984, MNRAS 211, 375

Bennett P.D., Harper G.M., Brown A., Hummel C.A., 1996, ApJ 471, 454

Bennett, P.D., Brown A., Yang S., 1998, IAU Colloq. 170: Precise Stellar Radial Velocities. E61

Bertelli G., Bressan A., Chiosi C., Fagotto F., Nasi E., 1994, A&AS 106, 275

Blackwell D.E., Lynas-Gray A.E., 1994, A&A 282, 899

Claret A., Gimenez A., 1992, A&AS 96, 255

Clementini G., Gratton R.G., Carretta E., Sneden C., 1999, MNRAS 302, 22

Dravins D., Gullberg D., Lindegren L., Madsen S., 1999, In: Hearnshaw J.B., Scarfe C.D. (eds.) Precise Stellar Radial Velocities. ASP Conference Series, in press

Fuhrmann K., 1998, A&A 338, 161

Goriely S., Clerbaux B., 1999, A&A 346, 798

Harmanec P., 1998, A&A 335, 173

Huebner W.F., Merts A.L., Magee N.H., Argo M.F., 1977, Los Alamos Sci. Lab. Rept., LA-6760-M

Iglesias C.A., Rogers F.J., Wilson B.G., 1992, ApJ 397, 717

Kurucz R.L., 1979, ApJS 40, 1

Kurucz R.L., 1992, private communication

Lester J.B., Gray R.O., Kurucz R.L., 1986, ApJS 61, 509

Maeder A., Peytremann E., 1970, A&A 7, 120

Perryman M.A.C., Lindegren L., Kovalevsky J., et al., 1995, A&A 304, 69

Pols O.R., Tout C.A., Schröder K.-P., Eggleton P.P., Manners J., 1997, MNRAS 289, 869

Popper D.M., 1980, ARA&A 18, 115

Popper D.M., McAlister H.A., 1987, AJ 94, 700

Richichi A., Ragland S., Stecklum B., Leinert C., 1998, A&A 338, 527

Rocha-Pinto H.J., Maciel W.J., 1996, MNRAS 279, 447

Rocha-Pinto H.J., Maciel W.J., 1998, MNRAS 298, 332

Rogers F.J., Iglesias C.A., 1992, ApJ 401, 361

Schaller G., Schaerer D., Meynet G., Maeder A., 1992, A&AS 96, 269

Schröder K.-P., Pols O.R., Eggleton P.P., 1997, MNRAS 285, 696

VandenBerg D.A., 1985, ApJS 58, 711